

# Effects of a Cell Adhesion Molecule Coating on the Blasted Surface of Titanium Implants on Bone Healing in the Rabbit Femur

Jin-Woo Park, DDS, MSD<sup>1</sup>/Sang-Gu Lee, DDS, MSD<sup>2</sup>/Byung-Ju Choi, DDS, PhD<sup>3</sup>/Jo-Young Suh, DDS, PhD<sup>4</sup>

**Purpose:** One strategy to improve implant osseointegration is to control the quality of the bone reaction at the implant-bone tissue interface using an implant coated with biologically active substances. The purpose of this study was to investigate the effect of a tetra-cell adhesion molecule (T-CAM) coating composed of 4 cell-adhesion molecules—an arginine-glycine-aspartic acid (RGD) sequence, a proline-histidine-serine-arginine-asparagine (PHSRN) sequence, a tyrosine-histidine sequence (YH), and a glutamic acid-proline-aspartic acid-isoleucine-methionine (EPDIM)—on the rough-surfaced titanium implant on peri-implant bone formation in the rabbit femur with poor local bone conditions and minimal primary stability. **Materials and Methods:** Seven T-CAM-coated (blasted/T-CAM) and uncoated (blasted) implants with a rough surface (hydroxyapatite-blasted; Ra = 1.8  $\mu\text{m}$ ) were placed in slightly oversized beds of the metaphyses of the right and left femurs of 7 New Zealand White rabbits with light tactile pressure, and minimal primary stability was obtained. To evaluate the effects of T-CAM coating on the peri-implant bone healing response, histomorphometric analysis was performed 8 weeks after surgery. The 2 groups were compared using the Student t test, with a significance level of  $P < .05$ . **Results:** Compared to uncoated blasted implants at 8 weeks of healing, the blasted/T-CAM implants showed a significantly greater amount of bone-implant contact (BIC;  $P < .01$ ) and new bone formation in the zones 0 to 100  $\mu\text{m}$  and 0 to 500  $\mu\text{m}$  lateral to the implant surface ( $P < .05$ ) in the medullary space. **Conclusion:** The T-CAM coating on the rough-surfaced titanium implants significantly enhanced peri-implant bone formation in rabbit femurs with poor local bone condition. (More than 50 references) INT J ORAL MAXILLOFAC IMPLANTS 2007;22:533–541

**Key words:** cell adhesion molecule, dental implants, osseointegration, poor bone quality, rough surface, titanium

The predictability and long-term success rates of endosseous dental implants have been well documented, both in fully and partially edentulous patients.<sup>1–3</sup> It is well-known that long-term success is greatly affected by local bone conditions, such as bone quality and quantity.<sup>4–6</sup> Higher implant failure rates have been reported in areas of poor-quality bone such as the posterior maxilla.<sup>5</sup>

Numerous approaches have been tried to improve clinical results in poor local bone conditions and to shorten healing periods.<sup>5,7,8</sup> One of the strategies used to improve osseointegration is to enhance the quality of the early interaction of bone-forming cells with the implant surfaces. Many studies have been performed to examine coating the surfaces of biomaterials with biologically active substances such as bone morphogenetic proteins, collagen, fibronectin, or peptides related to cell adhesion to enhance bone formation at the interface.<sup>9–12</sup> These approaches make the bioinert metallic implant surfaces bioactive and therefore improve the quality of the bone tissue reaction at the bone-implant interface.

The immobilization of cell adhesion molecules on the implant surface is one component of these approaches. Many studies have suggested that cell attachment plays a dominant role in subsequent proliferation and differentiation. It has been suggested that peptides containing arginine-glycine-aspartic acid (RGD) motifs increase osteoblast adhesion and subsequent proliferation on implant surfaces.<sup>13,14</sup>

<sup>1</sup>Assistant Professor, Department of Periodontology, College of Dentistry, Kyungpook National University, Daegu, Korea.

<sup>2</sup>Graduate Student, Department of Periodontology, College of Dentistry, Kyungpook National University, Daegu, Korea.

<sup>3</sup>Professor, Department of Dental Pharmacology, College of Dentistry, Kyungpook National University, Daegu, Korea.

<sup>4</sup>Professor, Department of Periodontology, College of Dentistry, Kyungpook National University, Daegu, Korea.

**Correspondence to:** Dr Jo-Young Suh, Department of Periodontology, College of Dentistry, Kyungpook National University, 188-1, Samduk 2Ga, Jung-Gu, Daegu, 702-412, South Korea. Fax: + 82 53 427 3263. E-mail: jysuh@mail.knu.ac.kr

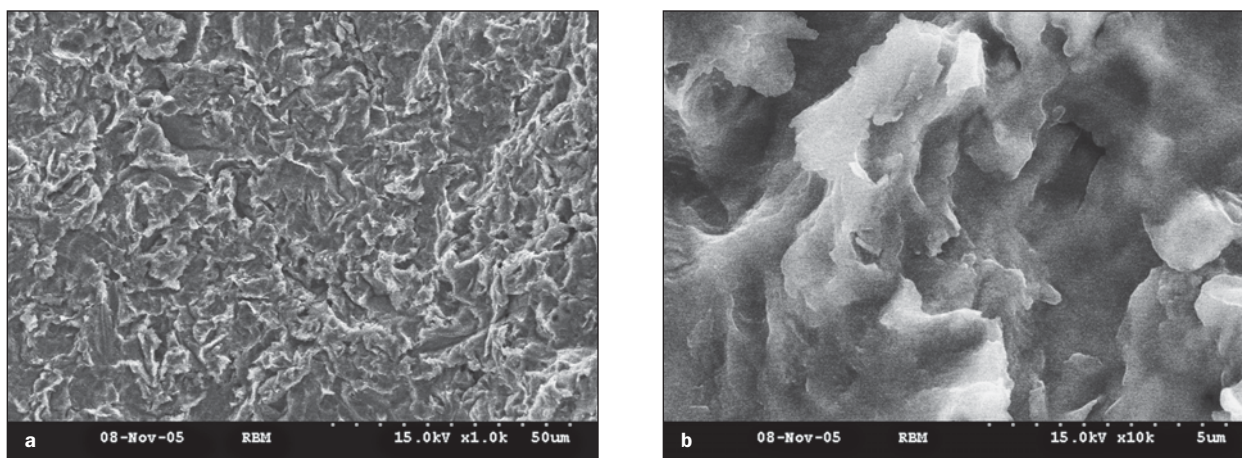


**Fig 1** Hydroxyapatite-blasted implants viewed with a scanning electron microscope (SEM) at magnifications of (a)  $\times 1,000$  and (b)  $\times 10,000$ .

Recently, it was observed that tetra-cell adhesion molecules (T-CAM), which are cell adhesion molecules, enhanced the differentiation of osteoblastlike cells grown on anorganic bovine bone mineral (ABBM) (submitted, 2007). T-CAM is a recombinant protein containing the RGD sequence in the tenth type III domain, a proline-histidine-serine-arginine-asparagine (PHSRN) sequence in the ninth type III domain of fibronectin, and a tyrosine-histidine (YH) sequence and a glutamic acid-proline-aspartic acid-isoleucine-methionine (EPDIM) sequence in the fourth fas-1 domain of  $\beta$ ig-h3. The RGD sequence interacts with several cell-surface integrins, the major one being  $\alpha 5\beta 1$ ,<sup>15,16</sup> which indicates its efficacy in promoting osteoblast adhesion.<sup>13,14,17</sup> The PHSRN sequence within the ninth type III domain serves as a synergic site that enhances the binding affinity of the RGD sequence, and both the RGD and PHSRN sequences in T-CAM are recognized by integrin  $\alpha 5\beta 1$  on osteoblastlike cells.<sup>18,19</sup>  $\beta$ ig-h3 is a cell adhesion protein whose expression is highly induced by transforming growth factor- $\beta$  (TGF- $\beta$ ) in several cell types and which has 4 internal repeat domains named fas-1.<sup>20</sup>  $\beta$ ig-h3 promotes cell adhesion and spreading through EPDIM and YH sequences present in the fourth fas-1 domain.<sup>21,22</sup>

Recently, it was demonstrated that bone defects in rabbit calvaria grafted with ABBM coated with T-CAM showed a significant increase of new mineralized bone formation.<sup>23</sup> As T-CAM-coated ABBM enhanced new bone formation in vivo, it was expected that coating titanium implant surfaces with the cell adhesion molecule T-CAM might also improve peri-implant bone healing. Therefore, the purpose of this study was to investigate the effects of T-CAM coating on the surfaces of titanium implants on peri-implant bone formation in the rab-

bit femur. Additionally, the peri-implant bone healing reaction to T-CAM-coated and uncoated titanium implants with rough surfaces placed in poor quality bone under conditions with minimal primary stability was investigated.

## MATERIALS AND METHODS

### T-CAM Synthesis

Fibronectin cDNA fragments (restricted to the Nde I and Nsi I sites) generated by polymerase chain reaction were inserted into the EcoRV sites of the fourth fas-1 domain of  $\beta$ ig-h3.<sup>16</sup> Plasmid constructs encoding T-CAM were transformed into BL21 cells for expression. Overnight bacterial cultures were induced, and T-CAM was purified using nickel-nitrilotriacetic acid (Ni-NTA) resin (Qiagen, Chatsworth, CA) according to the manufacturer's recommendations.

Cylindric implants 8.0 mm in length, with a coronal diameter of 3.9 mm and an apical diameter of 3.7 mm (MegaGen, Kyungsan, Korea) were made of commercially pure titanium (American Society for Testing and Materials [ASTM] Grade 2), and the surfaces were roughened by hydroxyapatite blasting (particle size of 100  $\mu$ m). The implants were then passivated in nitric acid according to ASTM specification F-86 (blasted implant; Fig 1).

Titanium implants were immersed in phosphate-buffered saline (PBS), with 1 implant per milliliter of solution containing 100  $\mu$ g T-CAM, for 24 hours at room temperature with gentle shaking. This T-CAM concentration was shown in a previous study to promote the differentiation of osteoblastlike cells on T-CAM-coated surfaces. Following the immersion, each implant was washed 3 times in PBS to remove non-adherent molecules, then dried in a laminar airflow

chamber for 24 hours (blasted/T-CAM implant). The blasted/T-CAM implants were used as the experimental implants, and uncoated blasted implants were used as the control implants.

Based on stylus profilometry (Form Talysurf Series 2; Taylor Hobson, London, UK), titanium implants showed the same roughness ( $R_a$ ) value ( $1.8 \mu\text{m}$ ) before and after T-CAM coating. Roughness was measured longitudinally on the lateral surface of the implant (Fig 2). All implants were sterilized by gamma irradiation before use.

### Animals and Surgical Procedure

Seven adult male New Zealand White rabbits weighing 3 to 3.5 kg were used in this study. This experiment was approved by the Institutional Animal Care and Use Committee of Kyungpook National University Hospital, Daegu, Korea.

General anesthesia was induced by intramuscular injection of a combination of 1.3 mL of ketamine (100 mg/mL; Ketara, Yuhan, Korea) and 0.2 mL of xylazine (7 mg/kg body weight; Rompun, Bayer Korea, Korea). The medial surfaces of the femoral metaphyses were used as the surgical sites. The surgical areas were shaved, and the skin was washed with a mixture of iodine and 70% ethanol prior to surgical draping. Local anesthesia—1.0 mL of 2% lidocaine (1:100,000 epinephrine; Yuhan, Korea)—was used to control bleeding. The surgical sites were exposed with an incision through the skin, fascia, and periosteum at the medial surface of the femur using sterile surgical techniques.

The implant sites were prepared in the usual manner. A final drill diameter of 3.85 mm was used. All drilling procedures were carried out under profuse sterile saline irrigation. Each femur received 1 implant. Blasted/T-CAM experimental implants and uncoated control implants were alternately placed in the right and left femur. The implants were inserted using a specially designed seating instrument with positioning its working end into the internal hole of the implant and light tactile pressure (Fig 2). The seating instrument was pushed with gentle rotation by finger pressure until the implant was in its final position (ie, until the coronal surface of the implant protruded 0.5 mm above the cortical bone surface).

All implants penetrated the first bone cortex only. Because of this preparation technique, implants were placed in a slightly oversized bed; the bed was 0.15 mm oversized at the apical region, but the gap between the bone wall and the implant gradually decreased toward the coronal aspect of the implant. Therefore, minimal stability was obtained by engaging only the top portion of the implant. The apical part of the implant could be moved laterally by

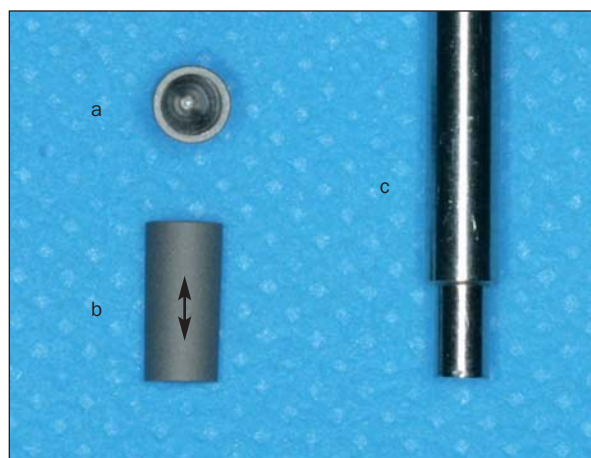


**Fig 2** (a) Superior and (b) lateral views of a blasted titanium implant alongside (c) the seating instrument. Arrow indicates the location and direction of surface roughness measurements.

applying a small force through the internal hole of the implant with an instrument tip.

After surgery, surgical sites were closed in layers and sutured using Vicryl (Ethicon, Somerville, NJ). Antibiotics (Baytril, Bayer Korea, Korea) and analgesics (Nobin, Bayer Korea, Korea) were injected intramuscularly for 3 days to prevent postsurgical infection and control pain. The animals were sacrificed by intravenous injection of air under general anesthesia at 8 weeks after surgery, and bone was prepared for histomorphometric evaluation.

### Specimen Preparation and Histomorphometric Evaluation

The distal femurs containing the implants were removed en bloc, fixed in 4% neutral buffered formaldehyde, dehydrated using an ascending series of alcohols, and embedded in methyl methacrylate for undecalcified sectioning. Undecalcified sections containing the central part of the implants were produced at a final thickness of  $20 \mu\text{m}$  using a Macro cutting and grinding system (Exakt 310 CP series; Exakt Apparatebau, Norderstedt, Germany). The sections were stained with Villanueva stain, and histomorphometric analysis was carried out using a light microscope (Axioplan 2; Carl Zeiss, Oberkochen, Germany) with an image analysis system (i-Solution, iMTechnology, Daejeon, Korea) under  $50\times$  magnification. Images were captured using a digital camera (AxioCam MRc 5; Carl Zeiss) attached to the microscope and displayed on a computer monitor.

Histometric measurements were performed to evaluate the following parameters:

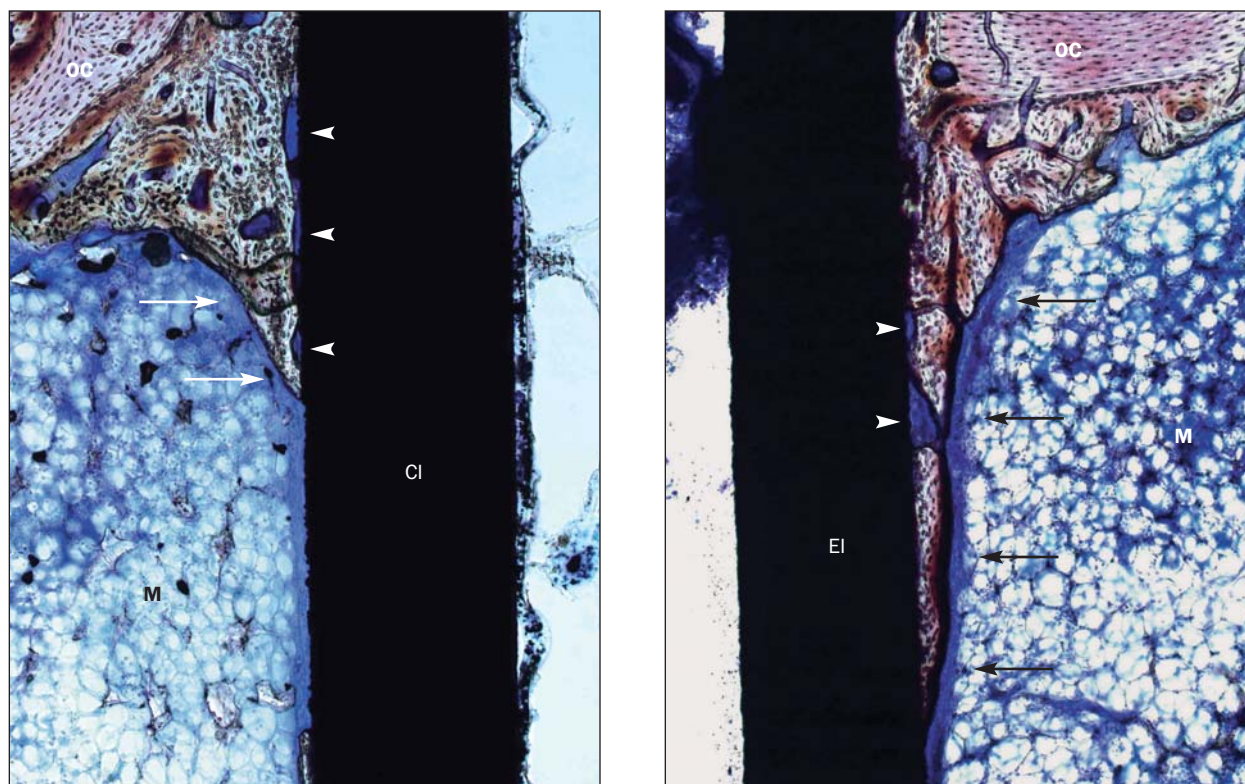


**Fig 3** Histologic sections of (left) control blasted and (right) experimental blasted/T-CAM implants in the marginal cortical bone region after 8 weeks of implantation. In the endosseous area, a greater amount of downward growth of newly formed bone tissue (arrows) from original cortical (OC) bone was observed on the surface of the experimental implant (EI) compared to the control implant (CI). Interruption of direct mineralized BIC (arrow head) was frequently observed on the surfaces of the blasted implants (CI) in the endosseous area. The medullary canal (M) lacks cancellous bone (Villanueva stain; bar equals 0.3 mm).

1. Bone-implant contact ratio (BIC %): BIC was measured as the percentage of the length of mineralized bone tissue in direct contact with the implant surface, out of the total length along the surface of the implant. BIC was then divided into 2 subclasses and represented as follows: (a) total BIC—percentage of the sum length of original cortical bone length and newly formed bone that were in direct contact with the implant, of the total length of the implant and (b) BIC in the medullary space—percentage of the length of newly formed mineralized bone tissue in the medullary space in direct contact with the implant, out of the total length of the implant in the medullary space.
2. Bone density in the medullary canal (BD %): The amount of newly formed mineralized bone tissue in the 0-to-100- $\mu$ m and 0-to-500- $\mu$ m zones adjacent to the lateral surface of the implant was measured. BD was calculated as the amount of mineralized bone tissue observed in each zone, out of the total area lateral to the surface of the implant (ie, as a percentage).

### Statistical Analysis

The histomorphometric data were processed with the SAS statistical system. The significance of differences between the 2 groups was analyzed using the Student *t* test. *P* values less than .05 were considered statistically significant.

## RESULTS

### Histologic Evaluation

Histologic evaluation showed an uneventful healing of all implants without any sign of inflammatory response. After 8 weeks of healing, implants were in contact with cortical bone along their upper portion, and new bone formation was observed in the marrow region, both in the blasted and blasted/T-CAM implants (Figs 3 to 5). The blasted/T-CAM implants showed greater downward growth of the newly formed mineralized bone tissue in the endosseous region compared to the blasted implants, while in the blasted implants, interruption of the direct con-

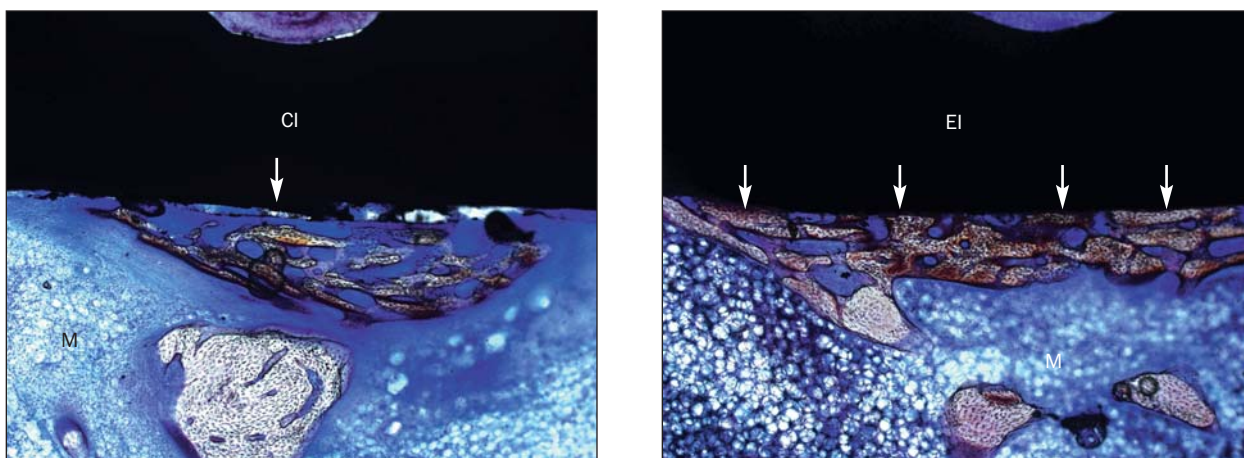


**Fig 4** New bone formation was observed in the apical region in both (*left*) blasted and (*right*) blasted/T-CAM implants. EI shows more frequent BIC (*arrows*) compared to CI (Villanueva stain; bar equals 0.5 mm).

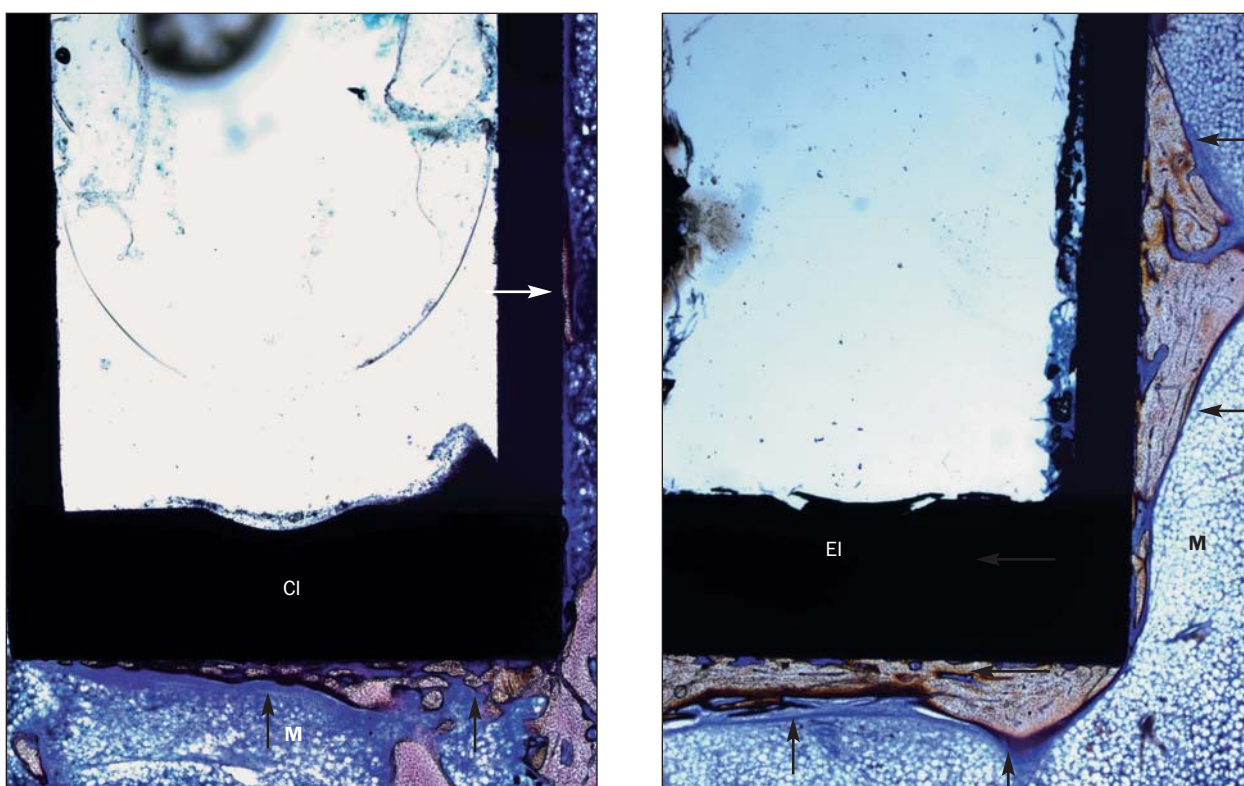


**Fig 5** Histologic sections of the apical part of (*left*) the control blasted and (*right*) experimental blasted/T-CAM implants placed in the medullary canal. A higher percentage of BIC and a greater amount of new bone formation can be observed around the EI compared to the CI. A thick, continuous layer of mineralized bone (*arrows*) can be observed along a large part of the implant surface. In contrast, a relatively thin and noncontinuous layer bone tissue (*arrows*) is present on the surface of the CI. More direct contact (greater BIC) was observed for the EI surface than for the CI surface (Villanueva staining; bar equals 1 mm).

tact between mineralized bone tissue and the implant surface was frequently observed in areas of newly formed bone in the endosseous region (Fig 3). The blasted/T-CAM implants showed more active bone formation, and a greater amount of mineralized bone tissue was observed in the apical area (Figs 4

and 5). A thick and continuous layer of newly formed bone tissue was observed around the blasted/T-CAM implants placed in the medullary canal, which was in direct contact with the implant surface, whereas less bone deposition was found with the control implants (Fig 5).

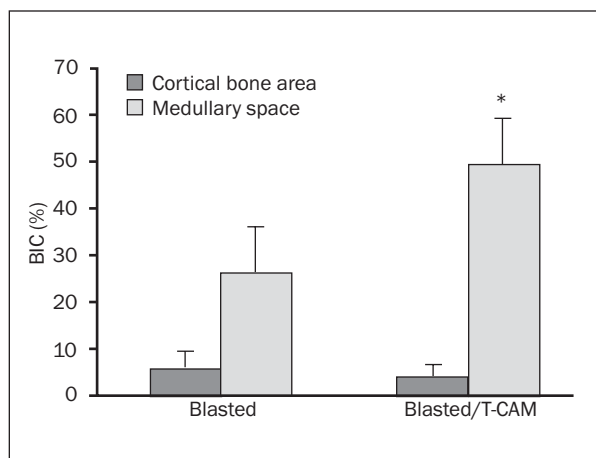


**Fig 6** Mean BIC percentage in the cortical region and in the medullary space after 8 weeks of healing. The BIC in the medullary space was significantly greater for the blasted/T-CAM implants compared to the blasted implants. \* $P < .01$ .

### Histomorphometric Analysis

The mean percentage of BIC was  $31.41\% \pm 8.52\%$  of the total area for the control implants and  $53.07\% \pm 10.87\%$  for the blasted/T-CAM implants. In the cortical region, the BIC was  $5.41\% \pm 3.98\%$  for blasted implants and  $3.94\% \pm 2.53\%$  for blasted/T-CAM implants. In the medullary space, the BIC was  $14.89 \pm 8.95\%$  for blasted implants, and  $49.14 \pm 9.98\%$  for blasted/T-CAM implants. The blasted/T-CAM implants showed a significantly greater mean BIC compared to the blasted implants in both the total area and medullary space ( $P < .01$ ; Fig 6).

The mean percentage of BD was significantly greater for blasted/T-CAM implants than for blasted implants in both the 0-to-100- $\mu\text{m}$  zone ( $45.06\% \pm 4.50\%$  vs  $24.97\% \pm 13.88\%$ ;  $P < .05$ ) and the 0-to-500- $\mu\text{m}$  zone ( $34.09\% \pm 7.93\%$  vs  $12.75\% \pm 11.93\%$ ;  $P < .05$ ).

## DISCUSSION

In this study, the authors investigated the effects of applying the cell adhesion molecule T-CAM to micro-roughened titanium implant surfaces on peri-implant bone formation with poor local bone conditions. The implants were placed in femoral metaphyses, which are characterized by a lack of cancellous bone. They were placed with minimal primary stability, achieved through slightly overdrilling of the implant sites. The blasted implants showed direct BIC in the cortical region and medullary space after 8 weeks of healing. The blasted/T-CAM implants showed significantly more BIC and new bone formation in the medullary space than the blasted implants.

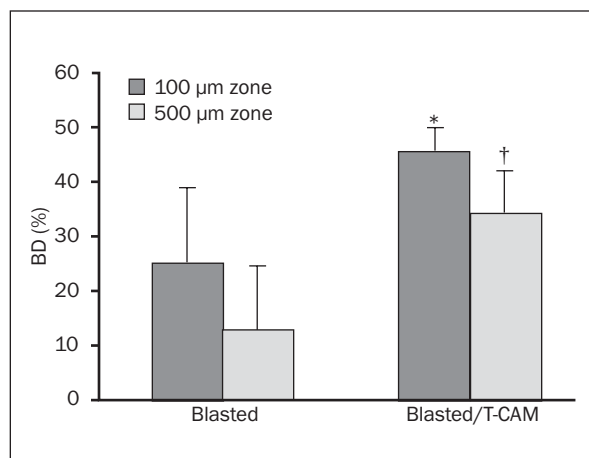


**Fig 7** Mean %BD in the medullary space. Mean %BD was significantly greater for the blasted/T-CAM implants than for the blasted implants in both the 0-to-100- $\mu\text{m}$  and 0-to-500- $\mu\text{m}$  zones (\* $P < .05$ , † $P < .05$ ).

Although the critical amount of BIC necessary to guarantee implant success has not been defined, Albrektsson and Johansson<sup>24</sup> suggested that approximately 50% BIC is necessary for functional loading of implants. Human histologic studies have shown various degrees of BIC with surface-modified implants either unloaded (30% to 96% BIC)<sup>25–27</sup> or after loading (25% to 83% BIC).<sup>28–31</sup> Numerous experimental studies have demonstrated a high degree of BIC; however, relatively high variation in BIC also has been reported.<sup>32–36</sup> In the canine mandible, significantly higher BIC (62.9%) was achieved with double acid-etched implants than with machined implants (39.5%) at 4 months, ( $P < .01$ ).<sup>32</sup> Ericsson et al<sup>33</sup> reported a similar value (65%) with TiO<sub>2</sub>-blasted implants; however, they measured BIC for the 3 best consecutive threads of the implants. In rabbit bone, 31% BIC at 3 months was achieved with TiO<sub>2</sub>-blasted implants in tibiae; fluoride modification increased BIC of blasted implants (39%).<sup>34</sup> Sul et al<sup>35</sup> achieved higher BIC (49%) for calcium ion-deposited titanium implants compared to machined implants (18%) at 6 weeks in rabbit tibia. Microroughened implants placed in femoral condyle of the goat, which is characterized by abundant cancellous bone, achieved relatively high percentages of BIC (51% at 6 weeks, 49% at 12 weeks).<sup>36</sup> When comparing the degree of BIC reported in the literature, the differences in experimental models, healing periods, and methods of measurement for histomorphometric analysis between studies should be considered. Differences in BIC% may be attributable to these variables.

Many studies have demonstrated the importance of primary stability to obtain successful osseointegration.<sup>6,37–40</sup> Higher initial stability may result from better local bone conditions, such as bone quality.

Lack of initial stability in poor-quality bone has resulted in lower implant success rates.<sup>37,38,40</sup> The degree of BIC achieved with hydroxyapatite-blasted implants (31.41%) in the present study corresponds to that achieved with TiO<sub>2</sub>-blasted implants (31%) placed in rabbit tibia at 3 months of healing; however, the TiO<sub>2</sub>-blasted implants were stabilized by relatively thick cortical bone.<sup>34</sup> Moreover, T-CAM coating significantly increased the BIC of blasted implants (53.07%). Several studies have shown that the amount of contact with cortical bone is more important for optimal implant stabilization than the amount of contact with trabecular bone.<sup>41,42</sup> Higher implant stability may result in increased BIC.<sup>43,44</sup> Direct comparison of bone healing in the rabbit and in clinical situations is naturally impossible, because conditions in experimental animals differ from those in humans. However, the present study provides evidence that a high degree of BIC can be achieved with hydroxyapatite-blasted implants in poor local bone conditions by applying T-CAM coating.

This study was predicated on the results of a previous animal experiment, which indicated that ABBM coated with T-CAM enhanced new bone formation in rabbit calvarial defects.<sup>23</sup> Numerous studies have shown that coating implant surfaces with bioactive substances such as growth factors or cell adhesion molecules influences the healing process at the bone-implant interface and thus can improve the quality and quantity of osseointegration.<sup>12,45-47</sup>

Adsorption of biomolecules, including proteins and peptides, onto solid surfaces is a very complicated process. It is well-known that many variables, including surface area, surface cleanliness, the concentration of the biomolecules, the buffer used, and the incubation time, can affect the process. However, it has been shown that most proteins adsorb irreversibly onto titanium surfaces because of the energetically favorable nature of the process.<sup>48</sup> A variety of complex immobilizing techniques have been studied for the covalent binding of biomolecules onto solid surfaces of biomaterials in attempts to overcome the disadvantages of simple adsorption, such as weak binding, conformational changes, denaturation, and subsequent loss of activity.<sup>12,49,50</sup> However, many *in vitro* studies have suggested that biomolecules immobilized by adsorption, for example, bone morphogenetic proteins, fibronectin, and TGF- $\beta$ 1, onto the surfaces of solid biomaterial including titanium retain their original biologic activity.<sup>9,10,46</sup>

The results of this *in vivo* study showed similar to the results attained in the aforementioned *in vitro* studies. T-CAM immobilized onto the surfaces of the titanium implants by simple adsorption, maintained its original activity, and thus, enhanced peri-implant

bone formation at the bone-implant interface by increasing bone-cell adhesion.

In this study, rough-surfaced implants were used to increase T-CAM adsorption. It has been reported that more protein is adsorbed onto rough titanium surfaces, which have more surface area than smooth surfaces, and that the amounts adsorbed increase with increasing protein concentration with a constant incubation time.<sup>51</sup> To the authors' knowledge, few studies have reported the peri-implant bone reaction in poor local bone conditions to implants with rough surfaces produced by hydroxyapatite blasting.

It is well-known that an increase in the implant surface area enhances biomechanical bonding by optimizing the biologic response of the bone and micromechanical interlocking.<sup>52-54</sup> Weng et al<sup>32</sup> demonstrated a significantly higher BIC rate for microroughened surfaces produced by double acid-etching compared with machined surfaces when placed in the "hollow part" of the canine mandible. The results of the present study were similar to their findings; hydroxyapatite-blasted surfaces showed frequent BIC and new bone formation in the apical area of the hollow medullary canal, indicating that the microroughened surface produced by hydroxyapatite blasting has advantages in sites of low bone content. In addition, more active bone formation and greater BIC were observed in T-CAM-coated implants compared to uncoated implants (Figs 4 and 5). The increased BIC and BD may have been due to the synergistic effects of the combination of the rough surface and the cell adhesion molecule, T-CAM.

The present results indicate that a T-CAM coating increases the osteoconductivity of microroughened implants placed in poor local bone conditions. The 4 cell-adhesion molecules of T-CAM enhance the regeneration potential of bone tissue at the interface by increasing adhesion of cells related to the bone formation process onto the implant surface and their subsequent proliferation and differentiation.

Although there are conflicting data on the distribution of integrins in osteoblasts, the fibronectin receptors  $\alpha$ 3 $\beta$ 1,  $\alpha$ 5 $\beta$ 1,  $\alpha$ v $\beta$ 3, and  $\alpha$ v $\beta$ 5 were localized to normal bone tissue, and  $\alpha$ 5 $\beta$ 1 has been identified in normal osteoblast cultures.<sup>55-58</sup> It has been reported that the RGD and PHSRN sequences in T-CAM are recognized by integrin  $\alpha$ 5 $\beta$ 1 on osteoblast-like cells.<sup>19</sup> The EPDIM sequence in T-CAM may be recognized by integrin  $\alpha$ 3 $\beta$ 1 in osteoblastlike cells, and the YH sequence may be recognized by integrin  $\alpha$ v $\beta$ 5 in such cells.<sup>21,22</sup>

Immobilization of T-CAM, composed of the cell-adhesion-related peptide sequences (-RGD-, -PHSRN-, -EPDIM-, -YH-), enhances peri-implant bone

formation by the synergistic effects of the combination of these 4 cell adhesion sequences, to increase osteoblast adhesion onto microroughened titanium implant surfaces. These results indicate that the cell adhesion molecule T-CAM increases the osteoconductivity of blasted titanium implants and that T-CAM can be effectively immobilized onto rough titanium implant surfaces by simple adsorption. In conclusion, T-CAM coating increased the regeneration potential of bone tissue at the bone-implant interface, improving the bone healing response to microroughened implants.

## CONCLUSION

Hydroxyapatite-blasted surfaces showed new bone formation and BIC in the hollow regions of the femur, and T-CAM coating on the hydroxyapatite-blasted surface of titanium implants significantly increased peri-implant new bone formation in rabbit femurs despite poor local bone conditions.

## ACKNOWLEDGMENTS

The authors wish to thank MegaGen, Korea, for providing the implants and Professor In-San Kim for providing the T-CAM used in this study.

## REFERENCES

- Adell R, Eriksson B, Lekholm U, Brånemark P-I, Jemt T. Long-term follow-up study of osseointegrated implants in the treatment of totally edentulous jaws. *Int J Oral Maxillofac Implants* 1990;5:347–359.
- Brocard D, Barthet P, Baysse E, et al. A multicenter report on 1,022 consecutively placed ITI implants: A 7-year longitudinal study. *Int J Oral Maxillofac Implants* 2000;15:691–700.
- van Steenberghe D, Lekholm U, Bolender C, et al. The applicability of osseointegrated oral implants in the rehabilitation of partial edentulism: A prospective multicenter study on 558 fixtures. *Int J Oral Maxillofac Implants* 1990;5:272–281.
- Esposito M, Hirsch JM, Lekholm U, Thomsen P. Biological factors contributing to failures of osseointegrated oral implants. (II). Etiopathogenesis. *Eur J Oral Sci* 1998;106:721–764.
- Khang W, Feldman S, Hawley CE, Gunsolley J. A multi-center study comparing dual acid-etched and machined-surfaced implants in various bone qualities. *J Periodontol* 2001;72:1384–1390.
- Morris HF, Ochi S, Orenstein IH, Petrazzuolo V. AICRG, Part V: Factors influencing implant stability at placement and their influence on survival of Ankylos implants. *J Oral Implantol* 2004;30:162–170.
- Buser D, Nydegger T, Oxland T, et al. Interface shear strength of titanium implants with a sandblasted and acid-etched surface: A biomechanical study in the maxilla of miniature pigs. *J Biomed Mater Res* 1999;45:75–83.
- Cochran DL, Buser D, ten Bruggenkate CM, et al. The use of reduced healing times on ITI implants with a sandblasted and acid-etched (SLA) surface: Early results from clinical trials on ITI SLA implants. *Clin Oral Implants Res* 2002;13:144–153.
- Itoh S, Matubara M, Kawauchi T, et al. Enhancement of bone ingrowth in titanium fiber mesh by rhBMP-2 and hyaluronic acid. *J Mater Sci Mater Med* 2001;12:575–581.
- Yang Y, Renee C, Ong JL. Protein adsorption on titanium surfaces and their effect on osteoblast attachment. *J Biomed Mater Res* 2003;67A:344–349.
- Geißler U, Hempel U, Wolf C, Scharnweber D, Worch H, Wenzel KW. Collagen type I-coating of Ti6Al4V promotes adhesion of osteoblasts. *J Biomed Mater Res* 2000;51:752–760.
- Schliephake H, Scharnweber D, Dard M, Sewing A, Aref A, Roessler S. Functionalization of dental implant surfaces using adhesion molecules. *J Biomed Mater Res B Appl Biomater* 2005;73:88–96.
- Rezania A, Healy KE. Integrin subunits responsible for adhesion of human osteoblastlike cells to biomimetic peptide surfaces. *J Orthop Res* 1999;17:615–623.
- Kantlehner M, Schaffner P, Finsinger D, et al. Surface coating with cyclic RGD peptides stimulates osteoblast adhesion and proliferation as well as bone formation. *Chembiochem* 2000;1:107–114.
- Pytela R, Pierschbacher MD, Ruoslahti E. Identification and isolation of a 140 kD cell surface glycoprotein with properties expected of a fibronectin receptor. *Cell* 1985;40:191–198.
- Ruoslahti E, Pierschbacher MD. New perspectives in cell adhesion: RGD and integrins. *Science* 1987;238:291–297.
- Verrier S, Pallu S, Bareille R, et al. Function of linear and cyclic RGD-containing peptides in osteoprogenitor cells adhesion process. *Biomaterials* 2002;23:585–596.
- Aota S, Nomizu M, Yamada KM. The short amino acid sequence Pro-His-Ser-Arg-Asn in human fibronectin enhances cell-adhesive function. *J Biol Chem* 1994;269:2456–2461.
- Krammer A, Craig D, Thomas WE, Schulten K, Vogel V. A structural model for force regulated integrin binding to fibronectin's RGD-synergy site. *Matrix Biol* 2002;21:139–147.
- Skonier J, Bennett K, Rothwell V, et al.  $\beta$ ig-h3: A transforming growth factor beta-responsive gene encoding a secreted protein that inhibits cell attachment in vitro and suppresses the growth of CHO cells in nude mice. *DNA Cell Biol* 1994;13:571–584.
- Kim J-E, Kim E-H, Han E-H, et al. A TGF- $\beta$ -inducible cell adhesion molecule,  $\beta$ ig-h3, is downregulated in melorheostosis and involved in osteogenesis. *J Cell Biochem* 2000;77:169–178.
- Kim J-E, Jeong H-W, Nam J-O, et al. Identification of motifs in the fasciclin domains of the transforming growth factor- $\beta$ -induced matrix protein  $\beta$ ig-h3 that interact with the  $\alpha$ v $\beta$ 5 integrin. *J Biol Chem* 2002;279:46159–46165.
- Lee J-H, Park J-W, Choi B-J, Kim I-S, Suh J-Y. Anorganic bone mineral coated with Tetra-Cell Adhesion Molecule enhances bone formation in rabbit calvarial defects. *Key Eng Mater* 2006;309:981–984.
- Albrektsson T, Johansson C. Quantified bone tissue reactions to various metallic materials with reference to the so-called osseointegration concept. In: Davies JE (ed). *The Bone-Biomaterial Interface*. Toronto: University of Toronto Press, 1991: 357–363.
- Iezzi G, Degidi M, Scarano A, Perrotti V, Piattelli A. Bone response to submerged, unloaded implants inserted in poor bone sites: A histological and histomorphometrical study of 8 titanium implants retrieved from man. *J Oral Implantol* 2005;31:225–233.



26. Ivanoff CJ, Hallgren C, Widmark G, Sennerby L, Wennerberg A. Histologic evaluation of the bone integration of TiO<sub>2</sub> blasted and turned titanium microimplants in humans. *Clin Oral Implants Res* 2001;12:128–134.
27. Lazzara RJ, Testori T, Trisi P, Porter SS, Weinstein R. A human histologic analysis of Osseotite and machined surfaces using implants with 2 opposing surfaces. *Int J Periodontics Restorative Dent* 1999;19:117–129.
28. Froum SJ, Simon H, Cho SC, Elian N, Rohrer MD, Tarnow DP. Histologic evaluation of bone-implant contact of immediately loaded transitional implants after 6 to 27 months. *Int J Oral Maxillofac Implants* 2005;20:54–60.
29. Hayakawa T, Kiba H, Yasuda S, Yamamoto H, Nemoto K. Histologic and histomorphometric evaluation of two types of retrieved human titanium implants. *Int J Periodontics Restorative Dent* 2002;22:164–171.
30. Romanos GE, Testori T, Degidi M, Piattelli A. Histologic and histomorphometric findings from retrieved, immediately occlusally loaded implants in humans. *J Periodontol* 2005;76:1823–1832.
31. Trisi P, Keith DJ, Rocco S. Human histologic and histomorphometric analyses of hydroxyapatite-coated implants after 10 years of function: A case report. *Int J Oral Maxillofac Implants* 2005;20:124–130.
32. Weng D, Hoffmeyer M, Hurzeler MB, Richter E-J. Osseotite vs machined surface in poor bone quality. *Clin Oral Implants Res* 2003;14:703–708.
33. Ericsson I, Johansson CB, Bystedt H, Norton MR. A histomorphometric evaluation of bone-to-implant contact on machine-prepared and roughened titanium dental implants. A pilot study in the dog. *Clin Oral Implants Res* 1994;5:202–206.
34. Ellingsen JE, Johansson CB, Wennerberg A, Holmen A. Improved retention and bone-to-implant contact with fluoride-modified titanium implants. *Int J Oral Maxillofac Implants* 2004;19:659–666.
35. Sul Y-T, Johansson CB, Albrektsson T. Oxidized titanium screw coated with calcium ions and their performance in rabbit bone. *Int J Oral Maxillofac Implants* 2002;17:625–634.
36. Vercaigne S, Wolke JGC, Naert I, Jansen JA. A histological evaluation of TiO<sub>2</sub>-gritblasted and Ca-P magnetron sputter coated implants placed into the trabecular bone of the goat: Part 2. *Clin Oral Implants Res* 2000;11:314–324.
37. Jemt T, Chai J, Harnett J, et al. A 5-year prospective multicenter follow-up report on overdentures supported by osseointegrated implants. *Int J Oral Maxillofac Implants* 1996;11:291–298.
38. Martinez H, Davarpanah M, Missika P, Celletti R, Lazzara R. Optimal implant stabilization in low density bone. *Clin Oral Implants Res* 2001;12:423–432.
39. Meredith N. Assessment of implant stability as a prognostic determinant. *Int J Prosthodont* 1998;11:491–501.
40. Glauer R, Ree A, Lundgren A, Gottlow J, Hammerle CH, Scharer P. Immediate occlusal loading of Brånemark implants applied in various jawbone regions: A prospective, 1-year clinical study. *Clin Implant Dent Relat Res* 2001;3:204–213.
41. Ivanoff CJ, Sennerby L, Lekholm U. Influence of mono- and bicortical anchorage on the integration of titanium implants. A study in the rabbit tibia. *Int J Oral Maxillofac Surg* 1996;25:229–235.
42. Sennerby L, Thomsen P, Ericson LE. A morphometric and biomechanic comparison of titanium implants inserted in rabbit cortical and cancellous bone. *Int J Oral Maxillofac Implants* 1992;7:62–71.
43. Nkenke E, Hahn M, Weinzierl K, Radespiel-Troger M, Newkam FW, Engelke K. Implant stability and histomorphometry: A correlation study in human cadavers using stepped cylinder implants. *Clin Oral Implants Res* 2003;14:601–609.
44. Lioubavina-Hack N, Lang NP, Karring T. Significance of primary stability for osseointegration of dental implants. *Clin Oral Implants Res* 2006;17:244–250.
45. Cochran DL, Schenk R, Buser D, Wozney JM, Jones AA. Recombinant human bone-morphogenetic protein-2 stimulation of bone formation around endosseous dental implants. *J Periodontol* 1999;70:139–150.
46. Fisher U, Hempel U, Becker D, et al. Transforming growth factor 1 immobilized adsorptively on Ti6Al4V and collagen type I coated Ti6Al4V maintains its biological activity. *Biomaterials* 2003;24:2631–2641.
47. Elmengaard B, Bechtold JE, Soballe K. In vivo effects of RGD-coated titanium implants inserted in two bone-gap models. *J Biomed Mater Res A* 2005;75:249–255.
48. Tengvall P. Proteins at titanium interfaces. In: Brunette DM, Tengvall P, Texter M, Thomsen P (eds). *Titanium in Medicine*. Berlin, Germany: Springer-Verlag, 2001:458–483.
49. Nanci A, Wuest JD, Peru L, et al. Chemical modification of titanium surfaces for covalent attachment of biological molecules. *J Biomed Mater Res* 1998;40:324–335.
50. Morra M, Cassinelli C, Cascardo G, et al. Surface engineering of titanium by collagen immobilization. Surface characterization and in vitro and in vivo studies. *Biomaterials* 2003;24:4639–4654.
51. Jansson E, Tengvall P. Adsorption of albumin and IgG to porous and smooth titanium. *Colloids Surf B Biointerfaces* 2004;35:45–51.
52. Davies JE. Mechanism of endosseous integration. *Int J Prosthodont* 1998;11:391–401.
53. Lossdorfer S, Schwartz Z, Wang L, et al. Microrough implant surface topographies increase osteogenesis by reducing osteoclast formation and activity. *J Biomed Mater Res A* 2004;70:361–369.
54. Szmukler-Moncler S, Perrin D, Bernard JP, Pointaire P. Biological properties of acid etched titanium surface. Effect of sandblasting on bone anchorage. *J Biomed Mater Res B Appl Biomater* 2004;15:149–159.
55. Brighton CT, Albelda SM. Identification of integrin cell substratum adhesion receptors on cultured rat bone cells. *J Orthop Res* 1992;10:766–773.
56. Clover J, Dodds RA, Gowen M. Integrin subunit expression by human osteoblasts and osteoclasts in situ and in culture. *J Cell Sci* 1992;103:267–271.
57. Hulthen K, Reinholt FP, Heinegard D. Distribution of integrin subunits on rat metaphyseal osteoclasts and osteoblasts. *Eur J Cell Biol* 1993;62:86–93.
58. Moursi AM, Damsky CH, Lull J, et al. Fibronectin regulates calvarial osteoblast differentiation. *J Cell Sci* 1996;109:1369–1380.